Intermolecular interactions between salmon calcitonin, hyaluronate and chitosan and their impact on the process of formation and properties of peptide-loaded nanoparticles

Anita Umerska, Owen I. Corrigan, Lidia Tajber*

School of Pharmacy and Pharmaceutical Sciences, Trinity College Dublin, Dublin 2, Ireland.

*To whom correspondence should be addressed: lidia.tajber@tcd.ie,

Phone: 00353 1 896 2787 Fax: 00353 1 896 2810

Abstract

The principal aim of this work was to study the formulation of a ternary complex comprising salmon calcitonin (sCT), hyaluronate (HA) and chitosan (CS) in a nanoparticle (NP) format. As interactions between the constituents are possible, their presence and component mass mixing ratio (MMR) and charge mixing ratio (CMR) were investigated to tune the properties of NPs.

Intermolecular interactions between sCT and HA as well as sCT and CS were studied by infrared spectroscopy (FTIR) and dynamic viscosity. The impact of MMR, CMR and HA molecular weight on the sCT loading capacity in NPs and *in vitro* release properties was determined.

sCT complexes to HA via electrostatic interactions and a support for hydrophobic interactions between sCT and HA as well as sCT and CS was found by FTIR. The sCT/HA complex is soluble but, depending on the mass mixing ratio between sCT and HA, NPs and microparticles were also formed indicative of associative phase separation between HA and sCT. The negatively charged HA/CS/sCT NPs were characterised by very high values (above 90%) of peptide association for the systems tested. Also, high sCT loading up to 50% were achieved. The peptide loading capacity and *in vitro* release properties were dependent on the NP composition. The zeta potential of the NPs without sCT was negative and ranging from -136 to -36 mV, but increased to -84 to -19 mV when the peptide was loaded. The particle size was found to be smaller and ranging 150-230 nm for sCT/NPs in comparison to NPs without sCT (170-260 nm). Short-term storage studies in liquid dispersions showed that the colloidal stability of NPs was acceptable and no release of sCT was observed for up to 3 days.

In conclusion, a range of NP systems comprising sCT, HA and CS was successfully developed and characterised. Such NPs may be considered as a suitable nanoparticulate format for the delivery of sCT.

KEYWORDS: hyaluronate, chitosan, salmon calcitonin, nanoparticles, polyelectrolyte complex, *in vitro* release

1. Introduction

Salmon calcitonin (sCT) is commercially available as an injectable and in a nasal spray form (Guggi et al., 2003). It is indicated for the treatment of bone diseases, e.g. osteoporosis, Paget's disease and bone metastasis (Guggi et al., 2003; Makhlof et al., 2010). sCT is also a promising candidate to be used in osteoarthritis (OA) (Manicourt et al., 2005) and in combined therapy with alendronate in patients with rheumatoid arthritis (RA) (Ozoran et al., 2007).

It has been reported that a major issue associated with development of efficient intra-articular (IA) delivery systems is the rapid clearance of many compounds from the joint (Morgen et al., 2013). Therefore it is desirable that such IA systems have a longer duration of action to minimise the number of injections due to the discomfort and pain associated with administration as well as possible risk of infection (Gerwin et al., 2006). A range of particulate carriers have been investigated to achieve this goal, including liposomes, microparticles (MPs) and nanoparticles (NPs) (Morgen et al., 2013). The use of MPs and NPs, e.g. albumin- or poly(lactic-co-glycolic acid) (PLGA)-based systems has been investigated (Gerwin et al., 2006). Horisawa et al., (2002) described that PLGA NPs should be more suitable for the delivery into the inflamed synovial tissue than MPs due to their ability to penetrate synovium. PLGA-based particles can provide local therapy actions in joint diseases in a different manner depending on the particle size (Horisawa et al., 2002). Other examples of sCT sustained release systems, but not indicated for IA delivery, include monolithic depot formulations prepared using lactide:glycolide copolymers (Millest et al., 1993), poly(ethylene glycol)-terephthalate and hydrophobic poly(butylene terephthalate) matrices (van Dijkhuizen-Radersmaet al., 2002) and PLGA microspheres incorporated into calcium phosphate cement (Zhong et al., 2012).

Hyaluronate (HA) is administered via the IA route in OA to help restore viscoelastic properties of synovial fluid (e.g. Synvisc injections), but HA has also been demonstrated to have a multiplicity of biological actions on cells *in vitro*, e.g. anti-inflammatory and direct anti-nociceptive effects (Gerwin et al., 2006). HA is also an ingredient of synovial fluid and it is known to interact with CD44 receptors of the cells, especially chondrocytes, playing an important role in functions of cartilage (Ishida et al., 1997). One of the attempts to increase the retention time of drugs within the knee cavity and to improve the interactions between cells and particles is the use of HA-functionalised poly(lactic acid)-PLGA particles (Zille et al., 2010).

When developing an effective nanoparticulate delivery system, the bioactive loading is a key parameter as often low loading limits the use of such systems, as a substantial amount of the formulation must be administered to achieve the therapeutic effect. This is a disadvantage of e.g. PLGA-based calcitonin NPs. Although the peptide can be very efficiently associated with particles, and for instance Yang et al. (2012) achieved up to 96.7% of loading efficiency, a very low peptide loading, ranging from 0.1 and 0.2% (Yang et al., 2012 and Glowka et al., 2010) to 1.55% (Kawashima et al., 2000) has been achieved. Other common disadvantages of lipid or PLGA-based NPs are the use of surfactants and organic solvents for their preparation. Cetin et al., (2012) produced Eudragit® and Eudragit®-PLGA NPs with a considerably higher sCT loading (up to 9.9%), but surfactants and organic solvents were used in their production, which may adversely affect the peptide stability and activity.

Polyelectrolyte complex NPs offer an attractive alternative, as they do not require organic solvents or surfactants in their manufacturing process. Makhlof et al., (2010) developed calcitonin-loaded NPs by the method of ionic gelation of chitosan (CS)-thioglycolic acid polymer conjugate with tripolyphosphate. Although the process of particle

preparation is simple and organic solvent free, the use of a novel polymer raises the need for complicated toxicity studies. Therefore employment of polymers already approved for the use in drug delivery provides an attractive option.

We have recently presented studies on a sCT-based nanocomplex able to reduce experimental inflammatory arthritis when delivered intra-articularly in an osteoarthritic murine *in vivo* model (Ryan et al., 2013). The nanocomplex was prepared by polyelectrolyte complex formation between HA, sCT and CS. The study of Ryan et al. (2013) clearly confirmed therapeutic efficacy and anti-inflammatory effects of sCT and HA by reducing nuclear receptor subfamily 4, group A, member 2 (NR4A2) mRNA expression *in vitro* as well as anti-arthritic effects *in vivo* following IA delivery. Having observed this interesting pharmacological response of sCT and HA we therefore decided to systematically study the formulation process on the properties of the sCT/HA/CS nanocomplex. The factors investigated included the component mass mixing ratio and HA molecular weight, while the characteristics studied comprised physical properties of NPs, their sCT loading and *in vitro* release properties. A possible complex formation between HA and sCT was proposed but not tested by Umerska et al. (2014) and this work presents the evidence and emphasises the implication of intermolecular interactions between the polyelectrolyte complex nanoparticle constituents.

2. Materials and methods

2.1 Materials

Hyaluronic acid sodium salt (HA) from *Streptococcus equi* sp. (sodium content of 3.6% w/w, Umerska et al. 2012) was purchased from Sigma (USA), while chitosan chloride (CS, molecular weight of 110±7 kDa, chloride residue content 16% and degree of deacetylation of ~83%, Umerska et al., 2012) was obtained from Novamatrix (Norway) as

Protasan UP CL113. Salmon calcitonin (sCT, as acetate salt) was obtained from PolyPeptide Laboratories (Denmark). All other reagents, chemicals and solvents were of analytical grade.

2.2 Preparation of HA/CS and HA/CS/sCT NPs

HA and CS solutions with concentrations of 0.1 or 0.2% w/v were prepared in deionised water. HA with molecular weights of 176, 257 and 590 kDa, later referred to as HA176, HA257 and HA590, respectively, were obtained by ultrasonication of native HA (2882±24.50 kDa) as previously described (Umerska et al., 2012). Briefly, processing of HA solutions was performed using a 130 W ultrasonic processor (SONICS VC130PB, Sonics and Materials Inc., USA) equipped with a probe with a diameter of 3 mm. Sonication was carried out at an amplitude of 80 (power of 13 W) on HA solutions contained in a beaker immersed in an ice bath.

NP carriers (NPs without sCT) were formed by adding a predefined aliquot of CS solution (pH 4) to a known volume of HA solution (pH 6), to form NPs with pre-defined HA/CS mass mixing ratios at room temperature under magnetic stirring. The stirring was maintained for 10 minutes to allow stabilisation of the system. A dispersion of particles was instantaneously obtained upon mixing of polymer solutions.

NPs containing sCT were formed following the above procedure. An appropriate quantity of the peptide, resulting in the final sCT concentration in the NP dispersion of 0.1, 0.2, 0.35, 0.5 and 1.0 mg/ml, was dissolved in the HA solution prior to mixing with the CS solution. The ratios reflecting the total number of negatively charged ionisable groups (n^-) to the total number of positively charged ionisable groups (n^+) were calculated considering the counterion content and the degree of deacetylation for chitosan and are presented in Table 2.

2.3 Characterisation and stability of NPs

2.3.1 Transmittance measurements

Transmittance of NP dispersions was measured using an UV-1700 PharmaSpec UV-Visible spectrophotometer (Shimadzu, Japan) at a wavelength of 500 nm in quartz cuvettes (Hellma, Germany) with the light path of 10 mm (Umerska et al., 2012).

2.3.2 Particle size and zeta potential analysis

The intensity-averaged mean particle size (hydrodynamic particle diameter) and the polydispersity index of the NPs were determined by dynamic light scattering (DLS) with 173º backscatter detection. The electrophoretic mobility values were measured by laser Doppler velocimetry (LDV) and converted to zeta potential using the Smoluchowski equation. DLS and LDV measurements were carried out on a Zetasizer Nano series Nano-ZS ZEN3600 fitted with a 633 nm laser (Malvern Instruments Ltd., UK) as described previously (Umerska et al., 2012). Samples, in their native dispersions, were placed into the folded capillary cells without dilution. Each analysis was carried out at 25 ºC with the equilibration time set to 5 minutes. The readings were repeated at least three times for each batch and the average values of at least three batches are presented. The results obtained were corrected for sample viscosity measured as described in Section 2.3.3.

2.3.3 Dynamic viscosity (DV)

Viscosity of samples was measured using a low frequency vibration viscometer (SV-10 Vibro Viscometer, A&D Company, Limited). Samples were equilibrated at 25 ºC in a water bath (Precision Scientific Reciprocal Shaking Bath Model 25) prior to the measurement. Three separate aliquots were prepared for each sample and at least three measurements were carried out for every aliquot.

2.3.4 Fourier transform infrared spectroscopy (FTIR)

HA and CS were first dissolved in deionised water at a concentration of 0.71 mg/ml and 5 ml of each solution was mixed with 5 ml of 1.09 mg/ml solution of sCT (made in deionised water) to achieve the polymer/sCT mass mixing ratio of 0.65. The aqueous

mixtures (HA, sCT/HA, CS and sCT/CS) were lyophilised as described previously (Umerska at el., 2012) and analysed using a Nicolet Magna IR 560 E.S.P. FTIR spectrophotometer. KBr discs with a 1% w/w sample loading were prepared by compression (4 bar for 1 minute). Accumulation of 64 scans and resolution of 2 cm^{-1} was used to obtain good quality spectra (Paluch et al., 2010). sCT was analysed as supplied.

2.3.5 Separation of non-associated sCT, association efficiency and peptide loading

Non-associated sCT was separated from NPs by a combined ultrafiltration-centrifugation technique (Centriplus YM-50, MWCO of 50 kDa, Millipore, USA) as described earlier (Umerska et al., 2014). A total of 5 ml of sample were placed in the sample reservoir (donor phase) of the centrifugal filter device and centrifuged for 1 hour at 3000 rpm. After centrifugation the volume of the solution in the filtrate vial (acceptor phase) was measured and the filtrate was assayed for the content of sCT by high-performance liquid chromatography (HPLC) as described in Section 2.3.7. This quantity of sCT was referred to as the non-associated sCT.

The NP suspension from the sample reservoir was made up to 5 ml with deionised water. 0.75 ml of the NP suspension from the sample reservoir was mixed with a predefined volume of 0.1 mM NaOH (this NaOH concentration was optimised and did not cause sCT degradation) to break up the NPs to release sCT and centrifuged for 30 minutes at 13,000 rpm. The supernatant was assayed for sCT content by HPLC (section 2.3.7). The rest of dispersion from the sample reservoir was analysed for signs of aggregation/destruction (by measuring mean particle size, zeta potential and transmittance).

The association efficiency (AE) and peptide loading (PL) were calculated with the use of the following equations:

$$AE = \left[\frac{A-B}{A}\right] * 100\% \quad \text{(Eq. 1)}$$

where A is the total amount (mass) of sCT and B is the mass of non-associated sCT

$$PL = \left[\frac{A-B}{C}\right] * 100\% \quad \text{(Eq. 2)}$$

where C is the total weight of all the components of NPs (the associated sCT and the mass of HA and CS used for the preparation of NPs).

2.3.6 Release studies

Aliquotes of 250 µl of NPs were added to 2.25 ml of phosphate buffered saline (PBS, pH=7.4). Samples were incubated at 37 ºC at 100 cpm in a reciprocal shaking water bath model 25 (Precision Scientific, India). After 1, 2, 4, 6 and 24 hours 2.5 ml aliquots were withdrawn and the released sCT was separated as described in Section 2.3.5. The samples were centrifuged at 4500 rpm for 15 minutes. After centrifugation the volume of the solution from the filtrate vial (acceptor phase) was measured and the filtrate was assayed for the content of sCT by HPLC (released sCT, Section 2.3.7). The NP suspension from the sample reservoir was made up to 2.5 ml with PBS and returned to the water bath to continue the release studies.

The data from release studies were fitted to the first order equation:

$$W = W_{\infty}(1 - e^{-kt}) \quad \text{(Eq. 3)}$$

where W is the amount of the peptide released at time t (based on cumulative release), W_{∞} is the amount of the peptide released at infinity and k is the release rate constant (Corrigan et al., 2006).

2.3.7 Quantification of sCT

Analysis of sCT content was performed using the HPLC system as described earlier (Umerska et al., 2014). Briefly, standard solutions of sCT (1.5–50 µg/ml) were prepared in deionised water and 50 µl of the standard or sample were injected onto the Jones Chromatography Genesis 4µ C18 150 × 4.6 mm column. The flow rate of 1 ml/min was used and the mobile phase was composed of 0.116% w/v NaCl, 0.032% v/v trifluoroacetic acid, and 34% v/v acetonitrile. The UV detection was carried out at 215 nm. The sCT peak had a

retention time of ~5 min. The concentration range of the calibration curve was 1.5–50 μg/ml, while the limit of detection and quantitation was 0.2 μg/ml and 0.7 μg/ml, respectively. Data collection and integration were accomplished using Shimadzu CLASS-VP software (version 6.10).

2.3.8 Physical stability of NPs

Physical stability studies of the NP native dispersions in water upon storage at room temperature were performed for a period of up to 3 days. Samples from each formulation were withdrawn periodically during the studies and the mean particle size, zeta potential and transmittance were measured as described in Sections 2.3.1 and 2.3.2.

2.3.9 Determination of the isoelectric point of NPs

The isoelectric point of NPs was determined by a Zetasizer Nano-ZS linked to a MPT-2 autotitrator (Malvern Instruments Ltd., UK). Amounts of 0.25M HCl and 0.25M NaOH were used as titrants and 12 ml of NP dispersion was added initially to the sample container. Each analysis was carried out at room temperature in automatic mode using the target pH tolerance of 0.2 units. Three particle size and three zeta potential measurements were carried out for each pH value and the sample was recirculated between repeat measurements.

2.4 Statistical analysis

The statistical significance of the differences between samples was determined using analysis of variance (ANOVA) followed by the posthoc Tukey's test using Minitab software. Differences were considered significant at $p<0.05$.

3. Results and discussion

3.1 Interactions in binary sCT/HA and sCT/CS systems

The estimated isoelectric point of sCT is 8.86 (Torres-Lugo and Peppas, 1999) and at pH 7.4 the peptide is expected to carry an overall charge of approximately 3+ (Epand et al., 1983). HA, on the other hand, with pKa of its carboxylic groups of 2.9 (Lapčik et al., 1998), bears a negative charge. As the protonated amino groups of proteins may associate with the de-protonated groups of anionic polysaccharides (de Kruif et al., 2004), both compounds, HA and sCT, are expected to interact by electrostatic forces at neutral and slightly acidic pH. This type of interactions may lead to associative phase separation through the formation of primary soluble macromolecular complexes (Doublier et al., 2000). On the other hand, intermolecular attraction based on charge between sCT and CS is unlikely as CS is a cationic polysaccharide with pKa of 6.5 (Boddohi et al., 2009).

To examine the possibility of sCT-polysaccharide complex formation, FTIR analysis was performed on sCT/HA and sCT/CS mixtures, prepared at a polysaccharide/sCT mass mixing ratio (MMR) of 0.65 (sample preparation is described in Section 2.3.4). The molecular weight of HA was 257 kDa (HA257), as this was found to be the optimum in the preparation of most of HA/CS NPs (Umerska et al., 2012). Fig. 1 shows the spectra (fingerprint region 650-1800 cm^{-1}) along with the assignment of principal absorption groups. Spectra of sCT/HA and sCT/CS systems were dominated by the absorption features of the polysaccharides even though sCT contributed a larger proportion of weight in the samples. Most changes in the FTIR spectra were observed in the region of vibrations associated with the 1,4-glycosidic ring of the polymers (950-1200 cm^{-1}) implying some hydrophobic interactions between sCT and the polymers (Sharon, 2006). However, alterations of the position of amide I band and the absorption of the $–COO^-$ group in HA were seen as well. Bands of HA initially at 1653, 1616 and 1567 cm^{-1} shifted to 1606, 1557 cm^{-1} (the peak at 1653 cm^{-1} is now present as a shoulder on the 1606 cm^{-1} band) consistent with the sCT and HA interactions electrostatic in nature.

Since FTIR studies showed that sCT may interact with HA via electrostatic bonds, the hypothesis of associative phase separation was subsequently tested as it has been reported that electrostatic interactions are typically the predominant types of interactions in associative mixed systems (Doublier et al. 2000). sCT and HA257 solutions were prepared and mixed at different ratios. The concentration of HA257 was kept constant (0.71 mg/ml) and different concentrations of sCT were used (0.54, 1.09, 1.63, and 2.17 mg/ml), equivalent to HA257/sCT MMRs of 1.3, 0.65, 0.44 and 0.33, and total n^-/n^+ charge mixing ratios (later referred to as CMRs) of 0.72, 0.96, 1.42 and 2.83, respectively. As summarised in Table 1, mixtures with HA257/sCT MMRs of 1.3 and 0.65 had the appearance of solutions, while mixtures containing HA257 and sCT at MMRs of 0.44 and 0.33 (sCT used in relatively large quantities) were turbid due to the formation of large particles, visible to the naked eye (supported by the low transmittance values). As the dispersion containing HA257/sCT at an MMR of 0.65 was slightly more turbid than a solution (Table 1), DLS and LDV measurements were performed to examine if NPs were formed. Although the measured particle size was 88±25 nm, the polydispersity index was high (0.65±0.19). Also, the zeta potential value was relatively low, -11.6±2.17 mV, indicating that although NPs were formed, they did not have good physical stability. The CMR appeared to be the main factor influencing the type of HA257/sCT dispersion. For CMRs greater than 1 (1.42 and 2.83) transparent systems indicating either the formation of soluble complexes or nanoparticles were obtained and for CMRs lower than 1 phase separation occurred.

To examine solubility of the particles formed when HA257 and sCT were mixed at MMRs of 0.44 and 0.33, the dispersions were diluted 1:1 (v/v) with water or 1:1 (v/v) with 1 mg/ml HA257 solution. In the latter case, the dilution resulted in an increase in the MMR from 0.44 to 0.87 (CMR 0.96 and 1.92) and from 0.33 to 0.65 (CMR 0.72 and 1.44). There was a dramatic decrease in absorbance for both samples upon dilution with the HA257

285 solution, a 14 and 22-fold for the samples with the initial MMR of 0.33 and 0.44,
286 respectively. Also, for both of the diluted liquids, absorbance was close to 0 (0.015±0.015
287 and 0.005±0.005 for the initial MMR of 0.33 and 0.44, respectively), therefore indicating that
288 the precipitate had practically dissolved. This is another confirmation that the CMR is the
289 main factor influencing appearance of HA/sCT dispersions. Following a 1:1 (v/v) dilution of
290 the particles with water, absorbance of HA257/sCT mixtures with MMRs of 0.44 and 0.33
291 decreased 4 and 3.2-fold, respectively.

292 Having observed that the precipitate formed when mixing HA257 and sCT solutions
293 at low MMR values was soluble in HA solution and that the formation of precipitate was
294 composition dependent, it was hypothesised that a soluble complex may also be formed. This
295 was investigated by measuring the dynamic viscosity (DV) of HA257 solution without and
296 with addition of sCT. After dissolving sCT in the HA257 solution the DV decreased
297 significantly ($p<0.05$) compared to the control (HA257 solution without sCT) (Fig. 2a). The
298 change in the DV values provides a confirmation that a soluble complex between HA257 and
299 sCT was formed. Interestingly, when sCT was dissolved in CS solution, the appearance of the
300 system did not change and the DV values of CS/sCT solutions did not differ from the
301 reference (CS solution without sCT) (Fig. 2b) for all CS concentrations tested.

302 In conclusion, infrared studies are consistent with the presence of hydrophobic
303 interactions between sCT and CS and sCT and HA. In the latter binary system there was
304 evidence of electrostatic interactions. sCT and HA appears to exhibit associative phase
305 separation as concluded from dynamic viscosity, transmittance and particle size data,
306 however only at certain HA257/sCT MMR values. Therefore, for studies involving formation
307 of HA257/CS/sCT systems, the HA257/sCT MMR ratio was always kept above 0.7 (Table 2)
308 to prevent the phase separation. As regards the HA257/CS/sCT preparative method, it was
309 decided that sCT would be dissolved in the HA257 solution to maximise interactions between

310 the species (due to solution pH and specific intermolecular interactions) and increase peptide
311 loading.

312 **3.2 Formation and characterisation of HA257/CS/sCT systems: impact of HA257/CS**
313 **mass mixing ratio (MMR), total polymer concentration and sCT concentration**

314 Observing that the HA257/sCT complex is soluble and even at high HA257/sCT
315 MMRs no particles with suitable physical properties were formed, a second polycation (CS)
316 was added to produce polyelectrolyte complex NPs containing sCT and HA. CS has been
317 shown to form an insoluble complex with HA (Denuziere et al., 2005; Umerska et. al 2012)
318 and it has been shown that in certain conditions the HA/CS complex is precipitated in the
319 form of NPs (Boddohi et al., 2009, Umerska et. al 2012).

320 Based on the results of previous studies (Umerska et. al 2012), a range of systems
321 with a total polysaccharide (HA257 and CS) concentration (TPC) of 1 mg/ml, HA257/CS
322 MMRs of 2.5, 5 and 10 with initial sCT concentration of 0.1, 0.2, 0.35, 0.5 and 1.0 mg/ml
323 were prepared. In most cases stable, non-sedimenting (within 24 hours or longer) NPs were
324 formed, however in formulations containing the highest concentration of sCT (1 mg/ml) and
325 HA257/CS MMRs of 2.5 and 5 (sample S15 and S14, respectively, Table 2) immediate
326 aggregation was observed. Furthermore, in the formulation with sCT concentration of 0.5
327 mg/ml and HA/CS MMR of 2.5 (sample S12, Table 2) precipitation was observed after a few
328 hours of storage at room temperature. All samples showing physical instability were
329 characterised by a CMR close to 1 (CMRs of 1.15, 1.26 and 0.94 for S12, S14 and S15,
330 respectively).

331 The next step was incorporation of high amounts of sCT (0.5 and 1.0 mg/ml) into NPs
332 with 2 mg/ml TPC and the same HA257/CS MMRs (2.5, 5 and 10). All formulations based
333 on HA257/CS MMRs of 5 and 10 were physically stable, no sedimentation was observed up
334 to 24 hours. In contrast to 1 mg/ml TPC NPs, the 2 mg/ml TPC-based formulation with a

HA257/CS MMR of 2.5 was physically stable and it was necessary to increase the concentration of sCT to 1 mg/ml to cause aggregation (sample S22, Table 2). Therefore the main factor determining the physical stability of HA257/CS/sCT NPs is not the HA/CS mixing ratio, but the mixing ratio of the three constituents. For instance, for HA257/CS NPs with MMR of 2.5 (TPC of 1 mg/ml), aggregation was observed for the HA257/CS/sCT formulation with an MMR of 2.5/1/1.75 (sample S12), while the formulation with TPC of 2 mg/ml and sCT of 0.5 mg/ml (a HA257/CS/sCT MMR of 2.5/1/0.87, sample S19) was stable. This is consistent with the CMR of sample S12 being closer to 1 (CMR=1.15) in comparison to sample S19 (CMR=1.27) and, when the concentration of sCT was increased to 1 mg/ml (sample S22), the CMR decreased to 1.11 and aggregation was observed.

Results presented in Section 3.1 and those published by Umerska et al., (2012) indicate that HA interacts with CS and sCT mainly by electrostatic forces and, as the negative charges of HA are neutralised by CS and sCT, the net charge of the particles decreases and aggregation occurs. Being positively charged in all the formulation conditions tested (pH of the NP dispersions containing sCT varied between 5.1 and 5.7), sCT and CS compete for binding with negatively charged carboxylic groups of HA. The interaction of CS with HA is expected to be stronger than the interaction between sCT and HA as CS is capable of precipitating HA at lower concentrations and has a higher charge density than sCT (Umerska et al., 2012).

As the measurements of transmittance and viscosity confirmed the formation of a binary HA257/sCT complex, these parameters were also measured for ternary HA257/CS/sCT systems. Transmittance values, which give information on the turbidity of samples, depend on the concentration and the particle size of NPs (Umerska et al., 2014). Transmittance of all 1 mg/ml TPC-based formulations decreased gradually with an increase in the amount of sCT used (Fig. 3). The difference was especially pronounced for NPs with a

360 HA257/CS MMR of 2.5. The decrease in transmittance values with increasing sCT
361 concentration was also observed for HA257/CS formulations with MMRs of 5 and 10 (Fig.
362 3). Similar to the binary HA257/sCT systems, the CMR influenced turbidity of the ternary
363 HA257/CS/sCT systems at the lower TPC (1 mg/ml). Samples with a CMR greater than 2
364 were transparent and a further decrease in the CMR from approximately 2 to 1.24 resulted in
365 a dramatic increase in turbidity of the samples. In contrast to NPs with a TPC of 1 mg/ml, it
366 was seen that when the TPC was increased to 2 mg/ml, the transmittance values of the
367 systems tested were not statistically significantly ($p<0.05$) different (Fig. 3). It can be
368 concluded that, in addition to effects of the HA257/CS MMR and TPC on dispersion
369 turbidity, incorporation of sCT has also an influence on transmittance. Rising turbidity values
370 corresponding to an increase in the sCT concentration may indicate that the binary complex
371 between sCT and HA did not fully dissociate after addition of CS and the peptide was
372 incorporated in the NPs. FTIR spectrum of a HA257/CS/sCT system (sample S9) was
373 dominated by absorption groups characteristic of the HA257/sCT complex (Fig. 1) with some
374 changes in intensity and position of bands located between 1500 and 1700 cm^{-1} and
375 previously reported as being distinctive of ionised carboxylic and amine groups of HA and
376 CS (Denuziere et al. 1996, Peniche et al. 2007, Lawrie et al. 2009 and Umerska et al. 2012).
377 It was seen for each HA257/CS MMRs and TPCs tested that inclusion of sCT
378 decreased the dynamic viscosity of the dispersions significantly (Fig. 4). The higher the dose
379 of sCT, the lower the dynamic viscosity of the liquid. This decrease in viscosity was the
380 greatest for formulations with a HA257/CS MMR of 10 and the smallest for a HA257/CS
381 MMR of 2.5-based formulations for both TPCs tested. As already stated by Umerska et al.,
382 (2012), the increased viscosity of colloidal dispersions compared to water may be attributed
383 to the free polymer present in the liquid. In all formulations tested here HA is believed to be
384 in excess and present either as free or loosely polymer bound to NP surfaces. As the NPs

385 themselves are not expected to have negligible effect on the viscosity (Philip et al., 1989),
386 HA appears to be the main factor determining the viscosity of the dispersions examined. As
387 presented above, the interaction between HA and sCT resulted in a decrease in the dynamic
388 viscosity of the liquid system and it may contribute to the decreased viscosity of the
389 HA257/CS dispersions.

390 In summary, the lower transmittance and viscosity values of ternary HA257/CS/sCT
391 systems compared with the binary HA257/CS samples confirm that in the ternary systems
392 interactions between sCT and HA are still present despite the competition between the positively
393 charged groups of CS and sCT for binding with the negatively charged groups of HA.

394 All HA257/CS NPs containing sCT were characterised by a small particle size, the
395 diameter of the particles was between 148±4 nm (TPC of 1 mg/ml; HA257/CS MMR of 5
396 and sCT of 0.35 mg/ml) and 229±28 nm (TPC of 1 mg/ml; HA257/CS MMR of 2.5 and sCT
397 of 0.35 mg/ml) (Fig. 5). These sizes are comparable to those measured for HA/protamine/sCT
398 NPs (100-500 nm, Umerska et al. 2014). Sizes of other sCT/NPs based on ionic complexation
399 reported so far are well over 200 nm in diameter. For example, Makhlof et al., (2010)
400 produced 245 nm glycol chitosan based NPs and Lee et al., (2010a) made TPP/sCT ionic
401 complex with the diameter of 225 nm. The lipid (Garcia-Fuentes et al., 2005) or PLGA NPs
402 (Yang et al., 2012) were also characterised by the particle size greater than 200 nm. However,
403 Cetin et al., (2012) obtained sCT-loaded Eudragit®-PLGA and Eudragit® NPs smaller than
404 200 nm (the smallest NPs had a diameter of 157±1 nm).

405 The incorporation of sCT decreased the diameter of the particles at HA257/CS MMRs of
406 5 and 10 (Fig. 5). A different behaviour was observed for formulations with a TPC of 1 mg/ml
407 and a HA257/CS MMR of 2.5 - employing up to 0.2 mg/ml sCT did not change the particle
408 size significantly, however a further increase in sCT concentration (to 0.35 mg/ml) resulted in
409 a statistically significant ($p=0.027$) increase in the particle diameter compared to the sample

without sCT. When a TPC of 2 mg/ml was employed to formulate NPs, only some of the sCT concentrations tested were seen to have an impact of the NP size (Fig. 5).

The increase in turbidity of NPs with a TPC of 1 mg/ml and containing larger amounts of sCT (Fig. 3), despite a decrease in the particle size (Fig. 5), suggests that more particles were formed in comparison to sCT-free NPs. An increase in the particle size of NPs with a TPC of 1 mg/ml, a HA257/CS MMR of 2.5 and sCT of 0.35 mg/ml was observed (sample S9, Table 2, Fig. 5). This formulation contains a relatively small excess of HA in relation to CS and sCT and it is possible that repulsion between the positively charged constituents in this sample (S9) due to their relatively smaller degree of neutralisation by negative charges of HA may be responsible for the increased particle size.

All NPs containing sCT were characterised by a narrow size distribution as the PDI values were in the range between 0.072±0.035 (TPC of 1 mg/ml, HA257/CS MMR of 2.5, sCT of 0.35 mg/ml) and 0.246±0.037 (TPC of 2 mg/ml, HA257/CS MMR of 10, sCT of 0.5 mg/ml) (Fig. 6). NPs with larger amounts of sCT were generally characterised by lower polydispersity than HA257/CS NPs without sCT (Fig. 6). The PDI values of HA257/sCT binary complexes were markedly higher than those observed for HA257/CS NPs or HA257/CS/sCT NPs. When making a ternary system composed of HA, CS and sCT it is possible that due to component interactions, in addition to a HA/CS/sCT complex, also HA/CS and HA/sCT NPs may form. The low PDI values observed for HA257/CS/sCT systems show that more uniform in size NPs formed and it is more likely to have only one type of the particles present – HA257/CS/sCT NPs.

All NPs tested had negative surface charge despite loading sCT into the particles (Fig. 7). A gradual increase in the zeta potential values was associated with the increase in sCT concentration used for prepare NPs. Nevertheless, most of the dispersions were characterised by the absolute values of zeta potential around 30 mV or greater, therefore indicating their

435 good physical stability. A statistically significant decrease in the surface charge can also be
436 linked to a decrease in the HA257/CS MMR and the TPC (Fig. 7). A linear relationship was
437 found when the zeta potential values were plotted as a function of CMR for both TPCs (R^2 of
438 0.9397 and 0.9644 for a TPC of 1 mg/ml and 2 mg/ml, respectively).

439 As shown in Table 2, the ratio of ionisable carboxylic groups in HA molecules to
440 ionisable amino groups in CS molecules does not correspond to the mass mixing ratio, as
441 both polymers have different charge density. As the actual number of the ionised groups also
442 depends on the environmental pH, HA (pKa 2.9) can be considered as fully dissociated at pH
443 between 5.1 and 5.7. At pH 5.7 approximately 86% of the amino groups of chitosan (pKa
444 6.5) are ionised, and when the pH decreases to 5.1 the ionisation degree increases to
445 approximately 96%.

446 Apart from the α-amino and α-carboxylic groups, the molecule of sCT contains other
447 amino acids with an ionisable side-chain: one carboxylic group of glutamic acid (pKa 4.07),
448 two ε-amino groups of lysine (pKa 10.53), one guanidinium group of arginine (pKa 12.48)
449 and one imidazole ring of histidine (pKa 6.10). Therefore the incorporation of sCT into the
450 HA/CS system has an important influence on the charge mixing ratio and the net positive
451 charge of sCT reduces the stoichiometric excess of the negative charges of HA (Table 2). It is
452 known that when the charge mixing ratio of polyelectrolyte complex NPs is close to 1,
453 aggregation and phase separation occurs (Boddohi et al., 2009, Umerska et al., 2012). The
454 experimental results show that samples with a total n^-/n^+ charge mixing ratio close to 1 (S12,
455 S15 and S22) were physically unstable. Interestingly, S14 (HA257/CS MMR 5, sCT 1.0
456 mg/ml) with a CMR of 1.26 was not stable, while S9 (HA257/CS MMR 2.5, sCT 0.5 mg/ml)
457 with a CMR of 1.24 was present as a stable colloidal dispersion. It may be due to the small,
458 but statistically significant difference in pH between those two formulations (Table 2) as the

amino groups of chitosan and the imidazole group of histidine in sCT will be ionised differently at these pH values.

In summary, analyses described in this Section confirmed that intermolecular interactions between negatively charged HA and positively charged CS and sCT are present in the ternary HA257/CS/sCT system and that sCT is incorporated within the NPs. The main factor determining the physical stability of HA257/CS/sCT NPs is the total n-/n+ charge mixing ratio. To obtain more information about the interactions in the complex, the quantitative analysis of sCT non-associated and associated with the NPs was performed and is described in Section 3.4.

3.3 HA/CS/sCT NPs - impact of molecular weight of HA

As presented by Umerska et al., (2012), the molecular weight (Mw) of HA had a considerable influence on the properties of HA/CS NPs. To investigate the influence of the molecular weight of HA on the properties of sCT-containing NPs, a formulation characterised by a HA/CS MMR of 5, a TPC of 1 mg/ml and sCT of 0.5 mg/ml was selected due to its good physical stability, small particle size (Fig. 5) and high sCT loading (sample S11, Table 2). Three molecular weights of HA were tested: 176 kDa (HA176), 257 kDa and 590 kDa (HA590). HA with a higher molecular weight was not considered due to formation of macroscopic aggregates with CS (Umerska et al., 2012).

Incorporation of sCT did not influence the turbidity of HA590 based formulations, however the transmittance of sCT-loaded NPs with HA176 and HA257 was significantly lower (77±4 and 70±8%, respectively) than their controls (NPs without sCT) (95±2 and 92±5%, respectively). The dynamic viscosity of dispersion containing sCT/NPs was significantly lower than that of the HA/CS NP dispersion without sCT for all three HA tested (Fig. 8A). HA590-based nano-suspension containing sCT/NPs was significantly more viscous in comparison to the other two formulations based on HA176 and HA257 (Fig. 8A).

The particle size of NPs containing HA with different Mw and 0.5 mg/ml sCT was lower than that of the respective controls (NPs without sCT), but only observed for HA590 ($p=0.019$) and HA257 ($p=0.041$) samples (Fig. 8B). All those sCT/NPs tested had similar particle sizes between 131-161 nm, which were not statistically different from each other, therefore it can be concluded that the molecular weight of HA in the range of ~150-600 kDa does not influence the particle size of sCT/NPs. The polydispersity index of sCT/NPs was lower compared with the control samples (Fig. 8C) and NPs based on HA590 were characterised by a significantly broader size distribution that NPs with HA176 and HA257.

The zeta potential values of the NPs were markedly higher for sCT/NPs when compared to the controls (NPs without sCT) (Fig. 8D). The difference in the zeta potential value between sCT/NPs and the control without sCT was the greatest for HA590-based NPs. Also, the value of zeta potential of this sample (loaded with sCT) was statistically significantly different compared to those of equivalent NPs comprising HA176 and HA257 ($p<0.01$).

3.4 sCT association efficiency and peptide loading

When preparing bioactive-containing NPs, it is necessary to determine the association efficiency (AE) and the bioactive loading, as they are two important NP quality control parameters with substantial impact in their application (Lu et al., 2011). Successful polymeric nanocarriers should be characterised by a high loading capacity in order to reduce the amount of the particles required for administration.

As shown in Table 2, sCT was associated with NPs very efficiently as in all formulations tested the AE values were well over 90%. Although there were statistically significant differences in the groups of formulations with a HA257/CS MMR of 5 and 10 when different concentrations of sCT were used (e.g. the AE of the sCT 0.5 mg/ml formulation was significantly lower ($p=0.041$) than the AE of other HA257/CS based

samples containing a smaller quantity of sCT), the differences were smaller than 2%, which is not expected to have any practical effect on properties of formulations. It is noteworthy that the formulations with the lowest AE for each HA257/CS MMR tested contained the highest dose of sCT for that particular HA257 and CS particle composition. It was observed that the HA257/CS MMR also had an effect on the AE of sCT in NPs. Although the difference was small, NPs with a HA257/CS MMR of 2.5 always had the AE value significantly lower than the two other MMRs for all concentrations of sCT tested ($p=0.022$, 0.001 and $p<0.001$ for 0.1, 0.2 and 0.35 mg/ml of sCT, respectively). The maximum amount of sCT which could be incorporated into the particles was determined by their composition - the more HA in the particles, the more sCT could be loaded in the NPs before aggregation occurred.

To summarise, sCT-loaded HA/CS NPs were characterised by an excellent association efficiency, which were consistently above 90% for all stable formulations made in contrast to HA/protamine/sCT NPs, where AE values were in the range 64-98% (Umerska et al., 2014). The system with the greatest peptide loading of 49.6% was that based on a 1 mg/ml TPC, a HA257/CS MMR of 10 and 1 mg/ml sCT (sample S13, Table 2). The high AE and DL values are undoubtedly a key advantage of HA257/CS NPs over many other NP-based delivery systems described so far. For instance, Vranckx et al. (1996) achieved sCT encapsulation efficiencies (EEs) of around 30-50% for butylcyanoacrylate nanocapsules, while sCT-loaded chitosan-coated lipid NPs formulated by Garcia-Fuentes et al. (2005) were characterised by EE values of 30-90%. PLGA NPs manufactured by Glowka et al., (2010) had peptide loading of 0.2% with EEs of 69-83% and NPs synthesised from a thiomer derivative of glycol chitosan and formed by ionic gelation with tripolyphosphate had AE values of 54-64% (Makhlof et al., 2010).

3.5 *In vitro* release of sCT from NPs

The results of *in vitro* release studies of sCT from NPs showed that the amount of sCT released within the first hour ranged between 23±4% (sample S9) and 54±4% (sample S7) (Fig. 9). The sample S9 (with 0.35 mg/ml of sCT and a HA257/CS MMR of 2.5) was characterised by a markedly lower peptide release than other formulations and only approximately 46% of sCT was released after 24 hours. Interestingly, this sample was made of HA257 and CS at an MMR of 2.5 indicating that the content of HA in this sample was low in comparison to a relatively high sCT content. In other formulations the amount of sCT released after 24 hours varied between 68 and 94%. Statistical comparisons (ANOVA) between the amounts of sCT released after 24 hours showed that sample S9 was different to samples S5, S7, S8 and S10.

The data from the release studies was fitted to the first order equation (Eq. 3). The parameter estimates and related statistics are summarised in Table 3. The k parameter (release rate constant) was found (by applying one-way ANOVA) to be independent of the dose of sCT loaded for the MMR of 10 ($p=0.778$) and the MMR of 2.5 ($p=0.764$), but not for the MMR of 5 ($p=0.002$). The MMR had no impact on the k parameter for NPs with 0.2 mg/ml sCT ($p=0.957$) and 0.35 mg/ml ($p=0.055$) but it was significant for 0.5 mg/ml sCT ($p=0.035$). The MMR had no impact on the W_∞ parameter (the amount of sCT released at infinity) for NPs with 0.2 mg/ml sCT ($p=0.058$) and 0.5 mg/ml sCT ($p= 0.543$), but it was significant for NPs with 0.35 mg/ml sCT ($p<0.001$). From Fig. 9 it appears that lower MMRs and higher amounts of sCT in NPs resulted in lower % of sCT released at 24h. Two-way ANOVA confirmed that this is, indeed, the case ($p<0.001$), however only the main effects (the MMR and sCT content) were significant ($p<0.001$ for both of parameters). Therefore there is no interaction (additive effect) between the MMR and sCT content parameters affecting the release properties of the NPs.

The release of sCT from HA257/CS NPs is relatively rapid, likely due to the electrostatic type of interactions between components and high solubility of the HA/sCT complex, compared with other delivery systems capable of providing the release of proteins for days (Corrigan and Li, 2009). Most likely, dissolution of NPs with concomitant release of the peptide occurs due to the high ionic strength of the release medium (PBS) with a contribution of sCT diffusion based of the concentration gradient. Fig. 9 and Table 3 show that less than 100% sCT was released from NPs in 24 h and it can be assumed that this amount of sCT remained complexed to HA. Differences is the amount of sCT released are seen for the various HA257/CS systems as described above in contrast to HA/protamine/sCT NPs (Umerska et al., 2014), where all systems studied had similar properties and released approximately 50% of the peptide in PBS after 1 hour of the studies. Therefore, when a slower peptide release is required, HA257/CS NPs might be a better formulation choice.

3.6 Stability studies of HA257/CS/sCT NPs

It is of importance to ensure that association of the drug with the NPs is unchanging upon storage and that degradation of the active does not occur prior to the conversion into a solid formulation, a more stable pharmaceutical format (Abdelwahed et al., 2006). No presence of non-associated/released sCT was observed after 1, 2 or 3 days of incubation, neither at 4 ºC, nor at room temperature (RT) or 37 ºC (Table 4), indicating that the sCT/NPs were stable in terms of peptide association. No major changes in the particle size, zeta potential and transmittance values were observed upon three days of storage, with the particle size increasing by ~4% for the batch stored at RT and at 37 ºC and transmittance values of the batch stored at 37 ºC decreasing on average by 11% (Table 4). However, PDI values of the sample changed by more than 10% on day three (storage at 4 and 20 ºC), suggesting that it is best to process the dispersions into powders within 48 h.

581 The HA257/CS MMR has been shown to be the main factor determining the
582 isoelectric point (IEP) of the particles (Umerska et al., 2012). The IEP values of HA257/CS
583 NPs (MMR=5 and TPC=1 mg/ml) containing different amounts of sCT (0.1, 0.2 and 0.5
584 mg/ml) was 2.42±0.07, 2.56±0.42 and 2.52±0.54, respectively. These values did not differ
585 significantly from the IEP of the reference formulation without sCT (IEP=2.47±0.25,
586 Umerska et al., 2012). These results suggest that sCT-loaded NPs are not expected to be
587 physically stable at low pH values, however they are likely to remain intact when
588 administered to the joints, as pH of synovial fluid is around 7 (Cummings and Nordby, 1996).
589

590 **4. Summary and conclusions**

591 This work shows that sCT is able to complex to HA via electrostatic interactions and
592 that evidence for hydrophobic interactions between sCT and HA as well as sCT and CS can
593 be inferred from infrared studies. The sCT and HA complex is soluble but, depending on the
594 charge mixing ratio between sCT and HA, the formation of NPs and MPs was observed
595 supporting the hypothesis of sCT/HA system exhibiting associative phase separation.

596 Ternary systems at the nanoscale comprising sCT, HA and CS were successfully
597 developed and characterised, a further development of previously presented binary HA/CS
598 systems (Umerska et al., 2012). The presence of all three components in these ternary
599 systems was confirmed by FTIR, peptide loading and release studies. The NPs were
600 spontaneously formed in mild conditions in a simple process of mixing aqueous
601 polyelectrolyte solutions at room temperature, without addition of any organic solvents
602 and/or surfactants. The negatively charged HA257/CS/sCT NPs were characterised by very
603 high values of peptide association, being all above 90% for the systems tested. Also, high
604 sCT loading up to 50% (w/w) were achieved. The loading capacity was dependent on the
605 composition of the NPs and increased with an increase in HA content in NPs. The sCT/NPs

were capable of providing a rapid release of sCT and modulation of peptide release was observed depending on the NP composition.

The presence of sCT in the NPs changed their physical properties when compared to the systems without sCT. The zeta potential of the particles increased due to the presence of sCT, however the particle size was found to be in general smaller for sCT/NPs. HA257/CS/sCT NPs had the hydrodynamic diameters ranging 150-230 nm, what makes them one of the smallest sCT NPs described so far. Moreover, short-term storage physical stability studies in liquid dispersions showed that the physical properties of the particles did not change and no leakage of sCT was observed for up to 3 days. In conclusion, the HA257/CS/sCT systems may be deemed as a suitable nanoparticulate carrier for the delivery of sCT.

Acknowledgments

This study was funded by the Irish Drug Delivery Research Network, a Strategic Research Cluster grant (07/SRC/B1154) under the National Development Plan co-funded by EU Structural Funds and Science Foundation Ireland. This work was also supported by the Synthesis and Solid State Pharmaceutical Centre funded by Science Foundation Ireland under grant number 12/RC/2275.

References

Abdelwahed, W., Degobert, G., Stainmesse, S., Fessi, H., 2006. Freeze-drying of nanoparticles: formulation, process and storage considerations. Adv. Drug Deliv. Rev. 58, 1688-1713.

629 Boddohi, S., Moore, N., Johnson, P., Kipper, M., 2009. Polysaccharide-based polyelectrolyte
630 complex nanoparticles from chitosan, heparin and hyaluronan. Biomacromolecules. 10, 1402-
631 1409.

632 Cetin, M., Aktas, M.S., Vural, I., Ozturk, M., 2012. Salmon calcitonin-loaded Eudragit® and
633 Eudragit®-PLGA nanoparticles: in vitro and in vivo evaluation. J. Microencapsul. 29, 156-
634 166.

635 Cooper, C.L., Dubin, P.L., Kayimazer, A.B., Turksen, S., 2005. Polyelectrolyte- protein
636 complexes. Curr. Opin. Colloid Interface Sci. 10. 52-78.

637 Corrigan, D.O., Healy, A.M., Corrigan, O.I., 2006. Preparation and release of salbutamol
638 from chitosan and chitosan co-spray dried compacts and multiparticulates. Eur. J. Pharm.
639 Biopharm. 62, 295-305.

640 Corrigan, O.I., Li, X., 2009. Quantifying drug release from PLGA nanoparticulates. Eur. J.
641 Pharm. Sci. 37, 477-485

642 Cummings, N.A., Nordby, G.L., 1966. Measurement of synovial fluid pH in normal and
643 arthritic knees. Arthritis Rheum. 9, 47-56.

644 de Kruif, C.G., Weinbreck, F., de Vries, R., 2004. Complex coacervation of proteins and
645 anionic polysaccharides. Curr. Opin. Colloid Interface Sci. 9, 340-349.

646 de la Fuente, M., Seijo, B., Alonso, M.J., 2008. Novel hyaluronan-based nanocarriers for
647 transmucosal delivery of macromolecules. Macromol. Biosci. 8, 441-450.

648 Denuziere, A., Ferrier, D., Domard, A., 1996. Chitosan-chondroitin sulfate and chitosan-
649 hyaluronate polyelectrolyte complexes. Physico-chemical aspects. Carbohydr. Polym. 29,
650 317-323.

651 Doublier, J.-L., Garnier, C., Renard, D., Sanchez, C. 2000. Protein-polysaccharide
652 interactions. Curr. Opin. Colloid Interface Sci., 5, 202-214.

653 Epand, R.M., Epand, R.F., Orlowski, R.C., Schlueter, R.J., Boni, L.T., Hui, S.W., 1983.
654 Amphipatic helix and its relationship to the interaction of calcitonin with phospholipids.
655 Biochemistry 22, 5074-5084.

656 Garcia-Fuentes, M., Torres, D., Alonso, M.J., 2005. New surface-modified lipid
657 nanoparticles as delivery vehicles for salmon calcitonin. Int. J. Pharm. 296, 122-132.

658 Gerwin, N., Hops, C., Lucke, A., 2006. Intraarticular drug delivery in osteoarthritis. Adv.
659 Drug Deliv. Rev. 58, 226-242.

660 Glowka, E., Sapin-Minet, A., Leroy, P., Lulek, J., Maincent, P., 2010. Preparation and in-
661 vitro- in vivo evaluation of salmon calcitonin loaded polymeric nanoparticles. J.
662 Microencapsul. 27, 25-36.

663 Guggi, D., Kast, C.E., Bernkop-Schnürch, A., 2003. In vivo evaluation of an oral salmon-
664 calcitonin delivery system based on a thiolated chitosan carrier matrix. Pharm. Res. 20, 1989-
665 1994.

666 Horisawa, E., Kubota, K., Tuboi, I., Sato, K., Yamamoto, H., Takeuchi, H., Kawashima, Y.,
667 2002. Size-dependency of DL-lactide/glycolide copolymer particulates for intra-articular
668 delivery system on phagocytosis in rat synovium. Pharm. Res. 19, 132-139.

669 Ishida, O., Tanaka, Y., Morimoto, I., Takigawa, M., Eto, S., 1997. Chondrocytes are
670 regulated by cellular adhesion through CD44 and hyaluronic acid pathway. J. Bone Miner.
671 Res. 12, 1657-1663.

672 Kamiya, N., Klibanov, A.M., 2002. Controlling the rate of protein release from
673 polyelectrolyte complexes. Biotechnol. Bioeng. 82, 590-594.

674 Kawashima, Y., Yamamoto, H., Takeuchi, H., Kuno, Y., 2000. Mucoadhesive DL-
675 lactide/glycolide copolymer nanospheres coated with chitosan to improve oral delivery of
676 elcatonin. Pharm. Dev. Tech. 5, 77-85.

677 Lapčík, L. Jr., Lapčík, L., de Smedt, S., Demeester, J., Chabreček, P., 1998. Hyaluronan:
678 preparation, structure, properties and applications. Chem. Rev. 98, 2664-2683.

679 Lawrie, G., Keen, I., Drew, B., Chandler-Temple, A., Rintoul, L., Fredericks, P., Grøndahl,
680 L., 2007. Interactions between alginate and chitosan biopolymers characterized using FTIR
681 and XPS. Biomacromolecules 8, 2533-2541.

682 Lee, H.E., Lee, M.J., Park, C.R., Kim, A.Y., Chun, K.H., Hwang, H.J., Oh, D.H., Jeon, S.O.,
683 Kang, J.S., Jung, T.S., Choi, G.J., Lee, S., 2010a. Preparation and characterization of salmon
684 calcitonin-sodium triphosphate ionic complex for oral delivery, J Control. Release. 143, 251-
685 257.

686 Lee, T.H., Cheng, W.T., Lin, S.Y., 2010b. Thermal stability and conformational structure of
687 salmon calcitonin in the solid and liquid states. Biopolymers. 93, 200-207.

688 Lu, X.-Y., Wu, D.-C., Li, Z.-J., Chen, G.-Q., 2011. Polymer Nanoparticles, in: Villaverde, A.
689 (Ed.), Nanoparticles in translational science and medicine, Academic Press, London, pp. 299-
690 323.

691 Makhlof, A., Werle, M., Tozuka, Y., Takeuchi, H., 2010. Nanoparticles of glycol chitosan
692 and its thiolated derivative significantly improved the pulmonary delivery of calcitonin. Int. J.
693 Pharm. 397, 92-95.

694 Manicourt, D.-H., Devogelaer. J.-P., Azria, M., Silverman, S., 2005. Rationale for the
695 potential use of calcitonin in osteoarthritis. J. Musculoskelet. Neuronal Interact. 5, 285-293.

696 Millest, A.J., Evans, J.R., Young, J.J., Johnstone, D., 1993. Sustained release of salmon
697 calcitonin in vivo from lactide: glycolide copolymer depots. Calcif. Tissue Int. 52, 361-364.

698 Morgen, M., Tung, D., Boras, B., Miller, W., Malfait, A.-M., Tortorella, M., 2013.
699 Nanoparticles for improved local retention after intra-articular injection into the knee joint.
700 Pharm. Res. 30, 257-268.

701 Ozoran, K., Yildirim, M., Önder, M., Sivas, F., Inanir, A., 2007. The bone mineral density
702 effects of calcitonin and alendronate combined therapy in patients with rheumatoid arthritis.
703 APLAR J. Rheumato. 10, 17-22.

704 Paluch, K.J., Tajber, L., McCabe, T., O'Brien, J.E., Corrigan, O.I., Healy A.M., 2010.
705 Preparation and solid state characterisation of chlorothiazide sodium intermolecular self-
706 assembly suprastructure. Eur. J. Pharm. Sci. 41, 603-611.

707 Peniche, C., Fernández, M., Rodríguez, G., Parra, J., Jimenez, J., Bravo, A.L., Gómez, D.,
708 San Román, J., 2007. Cell supports of chitosan/hyaluronic acid and chondroitin sulphate
709 systems. Morphology and biological behaviour, J. Mater. Sci. Mater. Med. 18, 1719-1726.

710 Philipp, B., Dautzenberg, H., Linow, K.J., Kötz, J., Dawydoff, W., 1989. Polyelectrolyte
711 complexes- recent developments and open problems. Prog. Polym. Sci. 14, 91-172.

712 Ryan, S.M., McMorrow, J., Umerska, A., Patel, H.B., Kornerup, K.N., Tajber, L., Murphy,
713 E.P., Perretti, M., Corrigan, O.I., Brayden, D.J., 2013. An intra-articular salmon calcitonin-
714 based nanocomplex reduces experimental inflammatory arthritis. J. Control. Release. 167,
715 120-129.

716 Sharon, N., 2006. Atomic basis of protein–carbohydrate interactions: an overview, in:
717 Bewley, C.A. (Ed.), Protein–carbohydrate interactions in infectious diseases, RSC
718 Publishing, Cambridge. pp. 1–5.

719 Torres-Lugo, M., Peppas N.A., 1999. Molecular design and in vitro studies of novel ph-
720 sensitive hydrogels for the oral delivery of calcitonin. Macromolecules. 32, 6646–6651.

721 Umerska, A., Paluch, K.J., Inkielewicz-Stępniak, I., Santos-Martinez, M.J., Corrigan, O.I.,
722 Medina, C., Tajber, L., 2012, Exploring the assembly process and properties of novel
723 crosslinker-free hyaluronate-based polyelectrolyte complex nanocarriers. Int. J. Pharm. 436,
724 75-87.

725 Umerska, A., Paluch, K.J., Santos-Martinez, M.J., Corrigan, O.I., Medina, C., Tajber, L.,
726 2014. Self-assembled hyaluronate/protamine polyelectrolyte nanoplexes: synthesis, stability,
727 biocompatibility and potential use as peptide carriers. J Biomed. Nanotechnol. 10, 3658-
728 3673.

729 van Dijkhuizen-Radersma, R., Nicolas, H.M., van de Weert, M., Blom, M., de Groot, K.,
730 Bezemer, J.M., 2002. Stability aspects of salmon calcitonin entrapped in poly(ether-ester)
731 sustained release systems. Int. J. Pharm. 248, 229-237.

732 Vranckx, H., Demoustier, M., Deleers, M., 1996. A new nanocapsule formulation with
733 hydrophilic core: Application to the oral administration of salmon calcitonin in rats. Eur. J.
734 Pharm. Biopharm. 42, 345-347.

735 Yang, M., Yamamoto, H., Kurashima, H., Takeuchi, H., Yokoyama, T., Tsujimoto, H.,
736 Kawashima, Y., 2012. Design and evaluation of poly(DL-lactic-co-glycolic acid)
737 nanocomposite particles containing salmon calcitonin for inhalation. Eur. J. Pharm. Sci. 46,
738 374-380.

739 Zhong, M.-L., Chen, X.-Q., Fan, H.-S., Zhang, X.-D., 2012. Incorporation of salmon
740 calcitonin-loaded poly(lactide-co-glycolide) (PLGA) microspheres into calcium phosphate
741 bone cement and the biocompatibility evaluation in vitro. J. Bioact. Compat. Pol. 27, 133 –
742 147.

743 Zille, H., Paquet, J., Henrionnet, C.J., Scala-Bertola, J.G., Leonard, M.J., Six, J.L.,
744 Deschamp, F., Netter, P., Verges, J., Gillet, P., Grossin, L., 2010. Evaluation of intra-articular

745 delivery of hyaluronic acid functionalized biopolymeric nanoparticles in healthy rat knees.
746 Bio-Med. Mater. Eng. 20, 235-242.

747 Figure captions

748 Figure 1. FTIR spectra of sCT, CS, sCT/CS, HA (as HA257), HA/sCT (containing HA as
749 HA257) and HA/CS/sCT (sample S9) systems. The mass mixing ratio between sCT and the
750 polysaccharide was 0.65 and the method of sample preparation is described in Section 2.3.4.
751 Band assignment was done based on studies of Denuziere et al. 1996, Peniche et al. 2007,
752 Lawrie et al. 2009, Lee et al. 2010b and Umerska et al. 2012. ν – stretching, $\nu_{s,a}$ – symmetric
753 and asymmetric stretching, ν_s – symmetric stretching and δ – bending vibrations.

754 Figure 2. Dynamic viscosity of a) HA and HA/sCT (HA as HA257) and b) CS and CS/sCT
755 liquid systems plotted against the polysaccharide concentration (mean ± S.D., n = 3). Lines
756 are for visual guide only.

757 Figure 3. Transmittance of empty (sCT 0.0 mg/ml) and sCT-loaded HA257/CS NPs. Non-
758 hashed bars indicate systems with TPC=1 mg/ml, hashed bars indicate systems with TPC=2
759 mg/ml. *$p<0.05$ and **$p<0.01$ versus sCT 0.0 mg/ml systems (mean ± S.D., n = 3).

760 Figure 4. Dynamic viscosity of empty (sCT 0.0 mg/ml) and sCT-loaded HA257/CS NPs.
761 Non-hashed bars indicate systems with TPC=1 mg/ml, hashed bars indicate systems with
762 TPC=2 mg/ml. *$p<0.05$, **$p<0.01$ and ***$p<0.001$ versus sCT 0.0 mg/ml systems (mean ±
763 S.D., n = 3).

764 Figure 5. Mean particle size of of empty (sCT 0.0 mg/ml) and sCT-loaded HA257/CS NPs.
765 Non-hashed bars indicate systems with TPC=1 mg/ml, hashed bars indicate systems with
766 TPC=2 mg/ml. *$p<0.05$ versus sCT 0.0 mg/ml systems (mean ± S.D., n = 3).

767 Figure 6. Polydispersity indices (PDI) of empty (sCT 0.0 mg/ml) and sCT-loaded HA257/CS
768 NPs. Non-hashed bars indicate systems with TPC=1 mg/ml, hashed bars indicate systems

769 with TPC=2 mg/ml. *p<0.05 and **p<0.01 versus sCT 0.0 mg/ml systems (mean ± S.D., n =
770 3).

771 Figure 7. Zeta potential (ZP) of empty (sCT 0.0 mg/ml) and sCT-loaded HA257/CS NPs.
772 Non-hashed bars indicate systems with TPC=1 mg/ml, hashed bars indicate systems with
773 TPC=2 mg/ml. *p<0.05, **p<0.01 and ***p<0.001 versus sCT 0.0 mg/ml systems (mean ±
774 S.D., n = 3).

775 Figure 8. Dynamic viscosity (top left), mean particle size (top right), polydispersity index
776 (PDI) (bottom left) and zeta potential (bottom right) of empty (sCT 0.0 mg/ml) and sCT-
777 loaded HA/CS NPs (sCT 0.5 mg/ml) containing HA with different molecular weights (M_w).
778 *p<0.05, **p<0.01 and ***p<0.001 versus sCT 0.0 mg/ml (mean ± S.D., n = 3).

779 Figure 9. Cumulative *in vitro* release profiles of sCT from sCT-loaded HA257/CS NPs. The
780 experiments were carried out using PBS (pH 7.4) at 37°C (mean ± S.D., n = 3). The
781 composition of samples is shown in Table 2.

Table 1 Characteristics of HA257/sCT mixtures with different mass mixing ratios. nHA – number of moles of disaccharide units of HA, nsCT – number of moles of sCT, n^- - anion, n^+ - cation, MMR – mass mixing ratio, CMR – charge mixing ratio. Each disaccharide unit of HA is composed of D-glucuronic acid and D-N-acetylglucosamine.

HA257/sCT MMR	nHA/nsCT	Total n-/n+ CMR	Visual appearance	Transmittance (%)	Presence of particulates/precipitation (size by DLS)
0.33	2.94	0.72	Turbid dispersion	62.2±2.3	Precipitate
0.44	3.92	0.96	Turbid dispersion	77.8±0.5	Precipitate
0.65	5.79	1.42	Transparent system	96.2±2.0	Nanoparticles, (mean size 88±25 nm)
1.30	11.59	2.83	Transparent system	99.6±0.1	No particles

Table 2 Association efficiency (AE) and sCT loading of HA257/CS/sCT NPs. Samples S12, S14 and S15 aggregated in the liquid and were not further analysed (N/A - data not available). TPC - total polysaccharide concentration, n^- - anion, n^+ - cation, MMR – mass mixing ratio, CMR – charge mixing ratio.

Sample	TPC (mg/ml)	HA conc. (mg/ml)	HA n- conc. (μmol/ml)	CS conc. (mg/ml)	CS n+ conc. (μmol/ml)	HA/CS MMR	HA/CS CMR	sCT conc. (mg/ml)	sCT n- conc. (μmol/ml)	sCT n+ conc. (μmol/ml)	Total n-/n+ CMR	pH	AE (%)	sCT loading (%)
S1	1	0.91	2.32	0.09	0.37	10	6.27	0.1	0.06	0.14	4.67	5.7±0.2	99.5±0.1	9.1±0.1
S2	1	0.83	2.12	0.17	0.71	5	2.99	0.1	0.06	0.14	2.56	5.6±0.0	99.5±0.3	9.1±0.1
S3	1	0.71	1.81	0.29	1.20	2.5	1.51	0.1	0.06	0.14	1.40	5.6±0.1	98.1±0.8	8.9±0.1
S4	1	0.91	2.32	0.09	0.37	10	6.27	0.2	0.12	0.27	3.81	5.4±0.0	99.5±0.3	16.6±0.1
S5	1	0.83	2.12	0.17	0.71	5	2.99	0.2	0.12	0.27	2.29	5.5±0.1	99.4±0.4	16.6±0.1
S6	1	0.71	1.91	0.29	1.20	2.5	1.59	0.2	0.12	0.27	1.38	5.4±0.1	96.0±1.0	16.1±0.2
S7	1	0.91	2.32	0.09	0.37	10	6.27	0.35	0.20	0.50	2.90	5.3±0.1	99.9±0.1	25.9±0.1
S8	1	0.83	2.12	0.17	0.71	5	2.99	0.35	0.20	0.50	1.92	5.3±0.1	99.6±0.1	25.9±0.1
S9	1	0.71	1.91	0.29	1.20	2.5	1.59	0.35	0.20	0.50	1.24	5.2±0.1	94.6±0.7	24.9±0.2
S10	1	0.91	2.32	0.09	0.37	10	6.27	0.5	0.29	0.72	2.39	5.2±0.1	99.9±0.1	33.3±0.1
S11	1	0.83	2.12	0.17	0.71	5	2.99	0.5	0.29	0.72	1.69	5.3±0.1	98.3±0.8	33.0±0.3
S12	1	0.71	1.91	0.29	1.20	2.5	1.59	0.5	0.29	0.72	1.15	5.2±0.1	N/A	N/A
S13	1	0.91	2.32	0.09	0.37	10	6.27	1.0	0.57	1.43	1.61	5.1±0.1	98.3±0.4	49.6±0.2
S14	1	0.83	2.12	0.17	0.71	5	2.99	1.0	0.57	1.43	1.26	5.1±0.0	N/A	N/A
S15	1	0.71	1.91	0.29	1.20	2.5	1.59	1.0	0.57	1.43	0.94	5.1±0.0	N/A	N/A
S17	2	1.82	4.64	0.18	0.75	10	6.19	0.5	0.27	0.72	3.34	5.3±0.0	99.6±0.1	19.9±0.1
S18	2	1.67	4.26	0.33	1.37	5	3.11	0.5	0.27	0.72	2.17	5.3±0.0	99.2±0.4	19.9±0.1
S19	2	1.43	3.64	0.57	2.36	2.5	1.54	0.5	0.27	0.72	1.27	5.2±0.3	94.2±1.9	19.1±0.4
S20	2	1.82	4.64	0.18	0.75	10	6.19	1.0	0.57	1.43	2.39	5.2±0.0	99.2±0.1	32.8±0.1
S21	2	1.67	4.26	0.33	1.37	5	3.11	1.0	0.57	1.43	1.73	5.1±0.1	97.7±0.4	33.3±0.1
S22	2	1.43	3.64	0.57	2.36	2.5	1.54	1.0	0.57	1.43	1.11	5.1±0.1	N/A	N/A

Table 3 Model parameter estimates (k - the release rate constant and W_∞ - the amount of sCT released at infinity) and related goodness of fit (R^2) statistics for sCT release data from HA257/CS NPs fitted to the first order model (Eq.3). The composition of samples is shown in Table 2.

Sample	k (h^{-1})	W_∞ (μg/mg of NPs)	R^2
S5	0.64±0.03	150±16	0.991
S6	0.65±0.22	109±11	0.997
S7	0.88±0.10	234±2	0.992
S8	0.86±0.02	232±7	0.994
S9	0.71±0.01	111±17	0.995
S10	0.92±0.10	247±10	0.997
S11	0.70±0.07	233±35	0.996
S13	0.97±0.22	404±8	0.997

Table 4 Physical stability studies of NPs with total polymer concentration (TPC) of 1 mg/ml, HA257/CS mass mixing ratio of 5 and 0.1 mg/ml of sCT (sample S2) – data presented as changes (%) to the starting values i.e. taking the data at day 0 as 100%.

	Temperature	Day 1	Day 2	Day 3
sCT associated with NPs	4 ºC	100.7±8.4	99.8±1.5	98.5±0.7
	20 ºC	98.1±5.5	100.5±2.2	98.6±0.1
	37 ºC	101.1±0.1	96.3±1.5	96.1±0.3
Transmittance	4 ºC	100.3±8.8	99.2±8.1	99.1±7.2
	20 ºC	101.1±8.4	98.6±7.4	100.9±4.2
	37 ºC	95.6±6.3	90.9±3.7	89.0±1.1
Mean particle size	4 ºC	100.3±0.3	99.7±1.1	99.4±3.4
	20 ºC	100.0±0.0	100.0±1.8	104.2±1.1
	37 ºC	101.7±0.2	99.3±0.4	103.6±0.1
Polydispersity index	4 ºC	92.2±9.4	96.4±6.9	88.9±8.3
	20 ºC	97.9±11.4	91.2±6.9	85.9±6.9
	37 ºC	91.3±9.9	92.1±4.8	98.4±7.9
Zeta potential	4 ºC	100.8±0.4	97.0±5.4	101.7±5.1
	20 ºC	100.5±1.7	100.2±11.7	94.4±4.8
	37 ºC	105.6±1.4	101.2±10.7	99.7±0.4

Figure 1. FTIR spectra of sCT, CS, sCT/CS, HA (as HA257), HA/sCT (containing HA as HA257) and HA/CS/sCT (sample S9) systems. The mass mixing ratio between sCT and the polysaccharide was 0.65 and the method of sample preparation is described in Section 2.3.4. Band assignment was done based on studies of Denuziere et al. 1996, Peniche et al. 2007, Lawrie et al. 2009, Lee et al. 2010b and Umerska et al. 2012. ν – stretching, $\nu_{s,a}$ – symmetric and asymmetric stretching, ν_s – symmetric stretching and δ – bending vibrations.

Figure 2. Dynamic viscosity of a) HA and HA/sCT (HA as HA257) and b) CS and CS/sCT liquid systems plotted against the polysaccharide concentration (mean ± S.D., n = 3). Lines are for visual guide only.

Figure 3. Transmittance of empty (sCT 0.0 mg/ml) and sCT-loaded HA257/CS NPs. Non-hashed bars indicate systems with TPC=1 mg/ml, hashed bars indicate systems with TPC=2 mg/ml. *p<0.05 and **p<0.01 versus sCT 0.0 mg/ml systems (mean ± S.D., n = 3).

Figure 4. Dynamic viscosity of empty (sCT 0.0 mg/ml) and sCT-loaded HA257/CS NPs. Non-hashed bars indicate systems with TPC=1 mg/ml, hashed bars indicate systems with TPC=2 mg/ml. *p<0.05, **p<0.01 and ***p<0.001 versus sCT 0.0 mg/ml systems (mean ± S.D., n = 3).

Figure 5. Mean particle size of of empty (sCT 0.0 mg/ml) and sCT-loaded HA257/CS NPs. Non-hashed bars indicate systems with TPC=1 mg/ml, hashed bars indicate systems with TPC=2 mg/ml. *p<0.05 versus sCT 0.0 mg/ml systems (mean ± S.D., n = 3).

Figure 6. Polydispersity indices (PDI) of empty (sCT 0.0 mg/ml) and sCT-loaded HA257/CS NPs. Non-hashed bars indicate systems with TPC=1 mg/ml, hashed bars indicate systems with TPC=2 mg/ml. *p<0.05 and **p<0.01 versus sCT 0.0 mg/ml systems (mean ± S.D., n = 3).

Figure 7. Zeta potential (ZP) of empty (sCT 0.0 mg/ml) and sCT-loaded HA257/CS NPs. Non-hashed bars indicate systems with TPC=1 mg/ml, hashed bars indicate systems with TPC=2 mg/ml. *p<0.05, **p<0.01 and ***p<0.001 versus sCT 0.0 mg/ml systems (mean ± S.D., n = 3).

Figure 8. Dynamic viscosity (top left), mean particle size (top right), polydispersity index (PDI) (bottom left) and zeta potential (bottom right) of empty (sCT 0.0 mg/ml) and sCT-loaded HA/CS NPs (sCT 0.5 mg/ml) containing HA with different molecular weights (M_w). *p<0.05, **p<0.01 and ***p<0.001 versus sCT 0.0 mg/ml (mean ± S.D., n = 3).

Figure 9. Cumulative *in vitro* release profiles of sCT from sCT-loaded HA257/CS NPs. The experiments were carried out using PBS (pH 7.4) at 37°C (mean ± S.D., n = 3). The composition of samples is shown in Table 2.

Figures – colour option

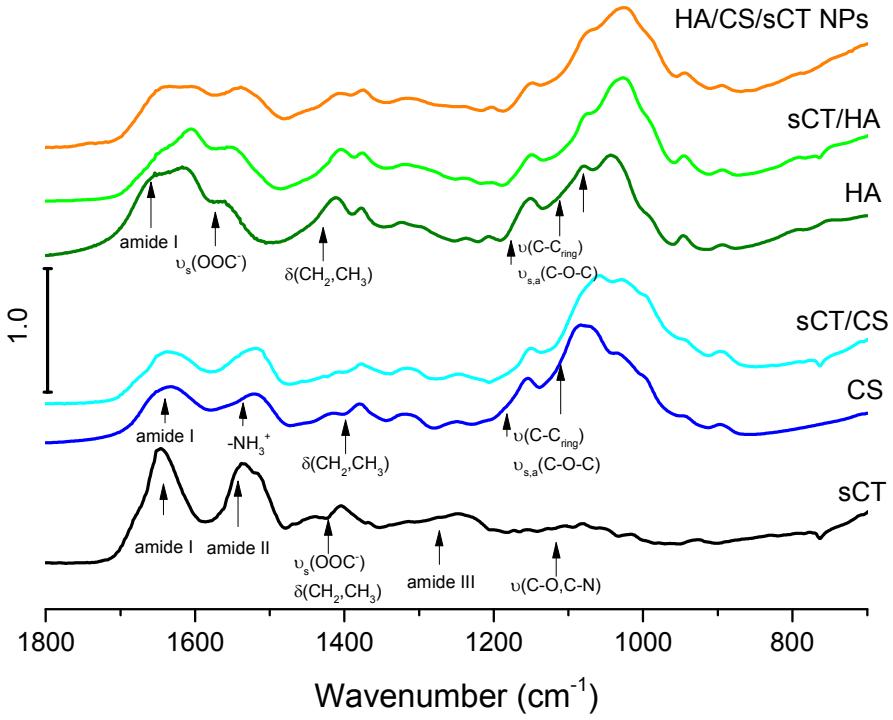

Figure 1.

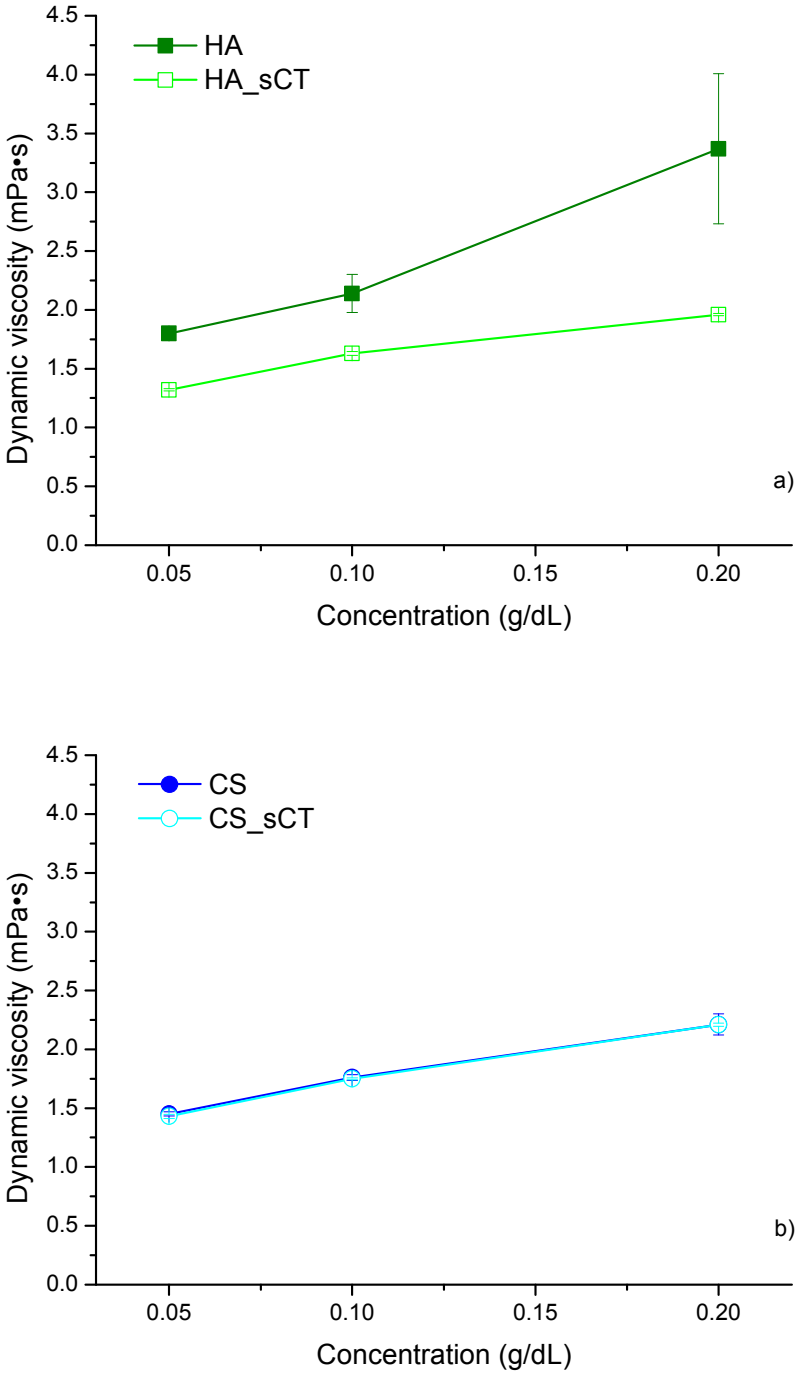
HA
HA_sCT
Dynamic viscosity (mPa•s)
Concentration (g/dL)
a)
CS
CS_sCT
Dynamic viscosity (mPa•s)
Concentration (g/dL)
b)

Figure 2.

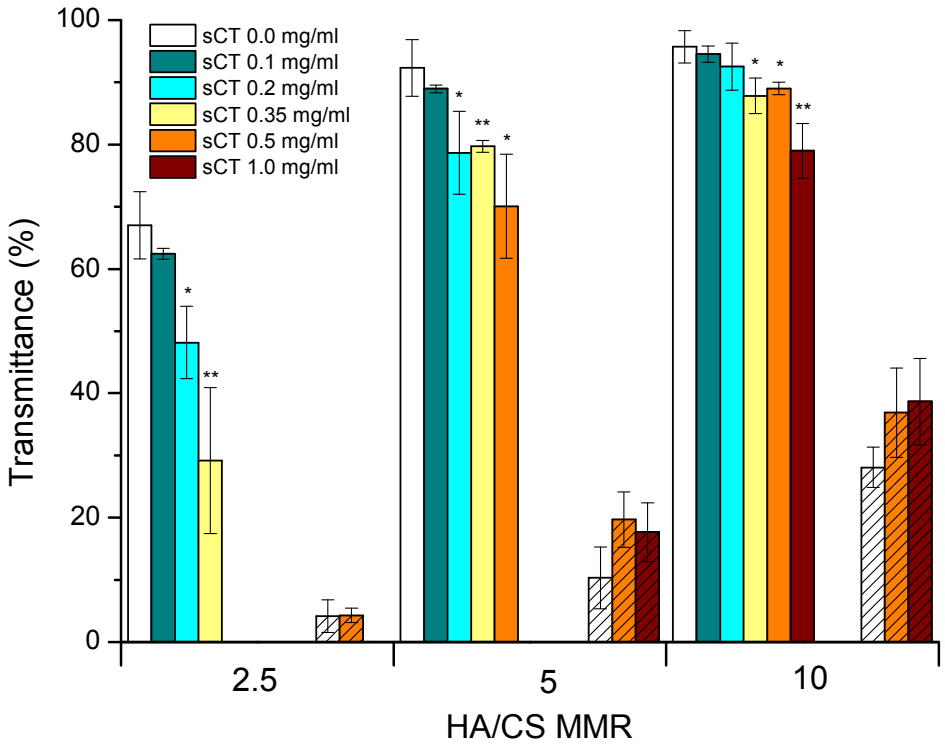
sCT 0.0 mg/ml
sCT 0.1 mg/ml
sCT 0.2 mg/ml
sCT 0.35 mg/ml
sCT 0.5 mg/ml
sCT 1.0 mg/ml
Transmittance (%)
100
80
60
40
20
0
2.5
5
10
HA/CS MMR

Figure 3.

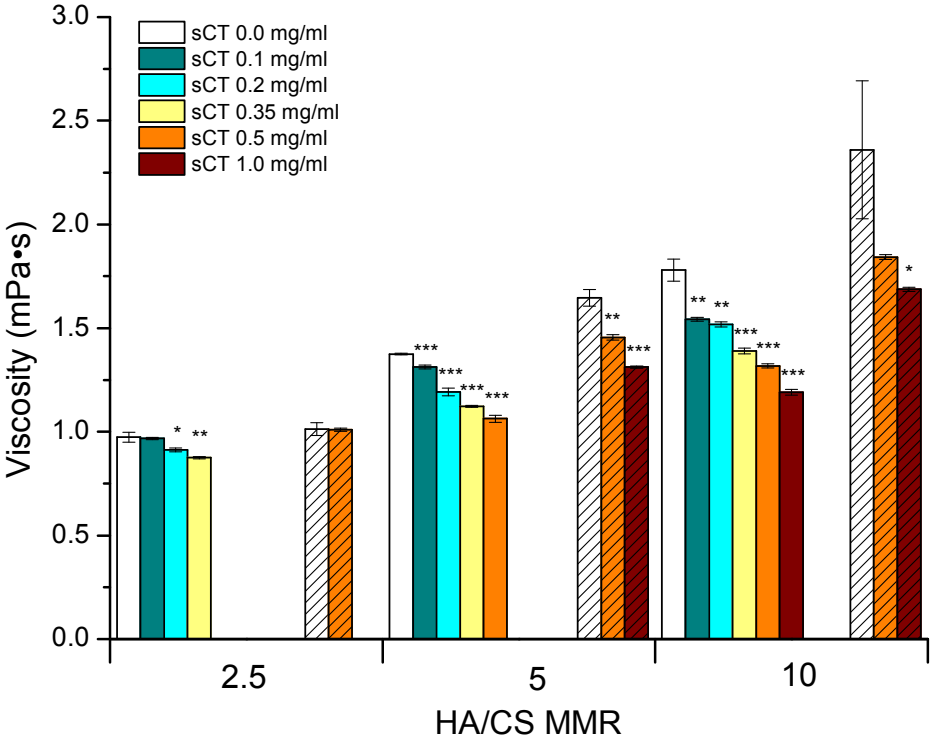
sCT 0.0 mg/ml
sCT 0.1 mg/ml
sCT 0.2 mg/ml
sCT 0.35 mg/ml
sCT 0.5 mg/ml
sCT 1.0 mg/ml
Viscosity (mPa•s)
3.0
2.5
2.0
1.5
1.0
0.5
0.0
2.5
5
10
HA/CS MMR

Figure 4.

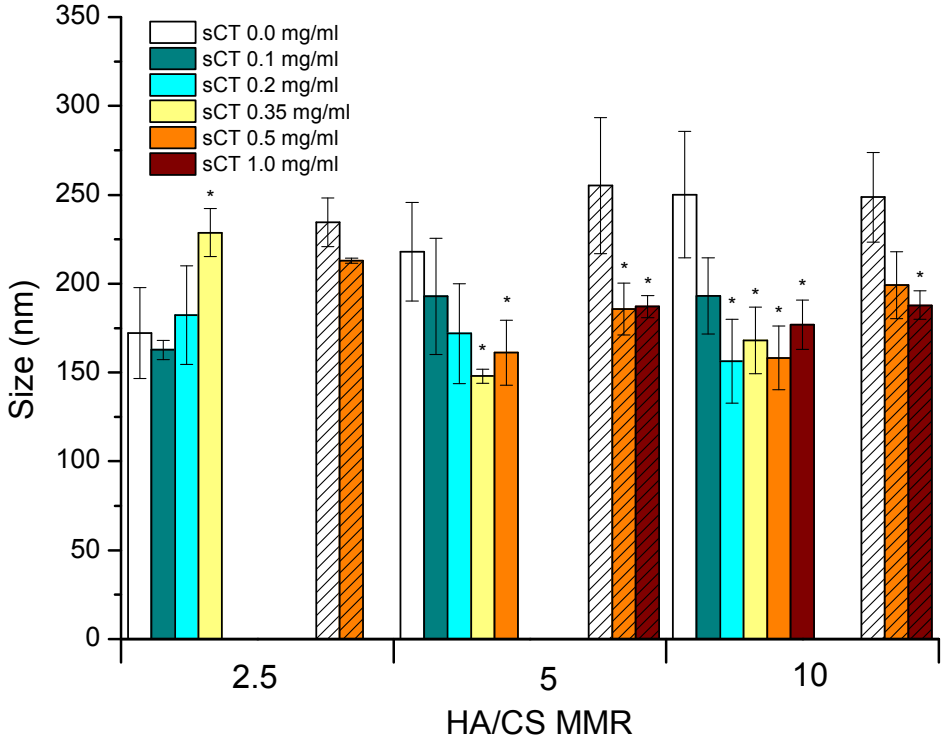
sCT 0.0 mg/ml
sCT 0.1 mg/ml
sCT 0.2 mg/ml
sCT 0.35 mg/ml
sCT 0.5 mg/ml
sCT 1.0 mg/ml
Size (nm)
350
300
250
200
150
100
50
0
2.5
5
10
HA/CS MMR

Figure 5.

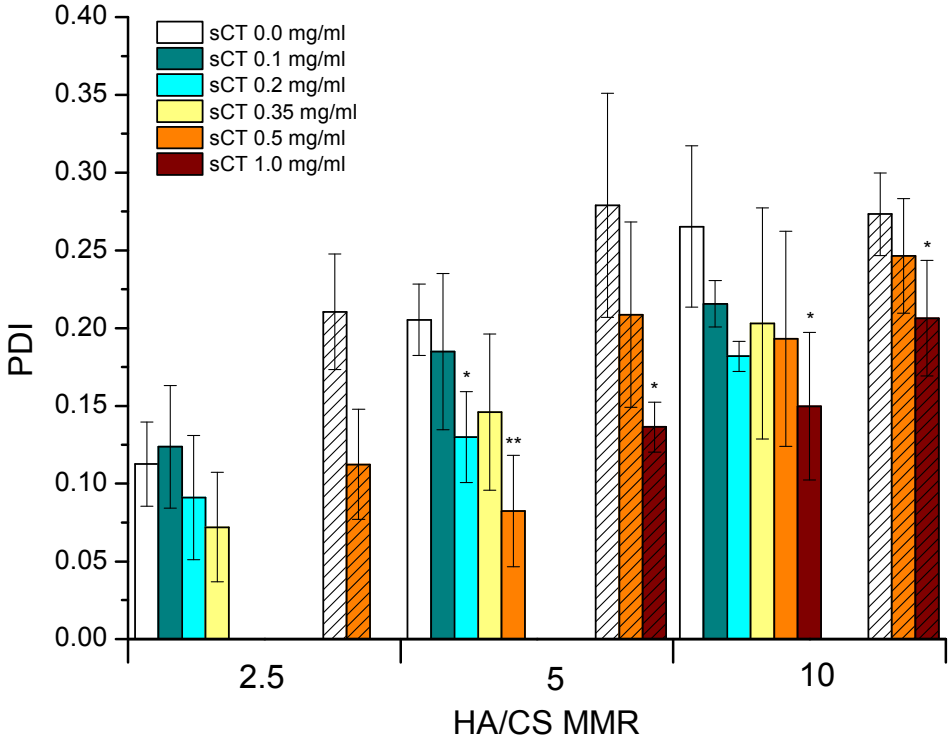
sCT 0.0 mg/ml
sCT 0.1 mg/ml
sCT 0.2 mg/ml
sCT 0.35 mg/ml
sCT 0.5 mg/ml
sCT 1.0 mg/ml
PDI
0.40
0.35
0.30
0.25
0.20
0.15
0.10
0.05
0.00
2.5
5
10
HA/CS MMR
*
**
*
*
*

Figure 6.

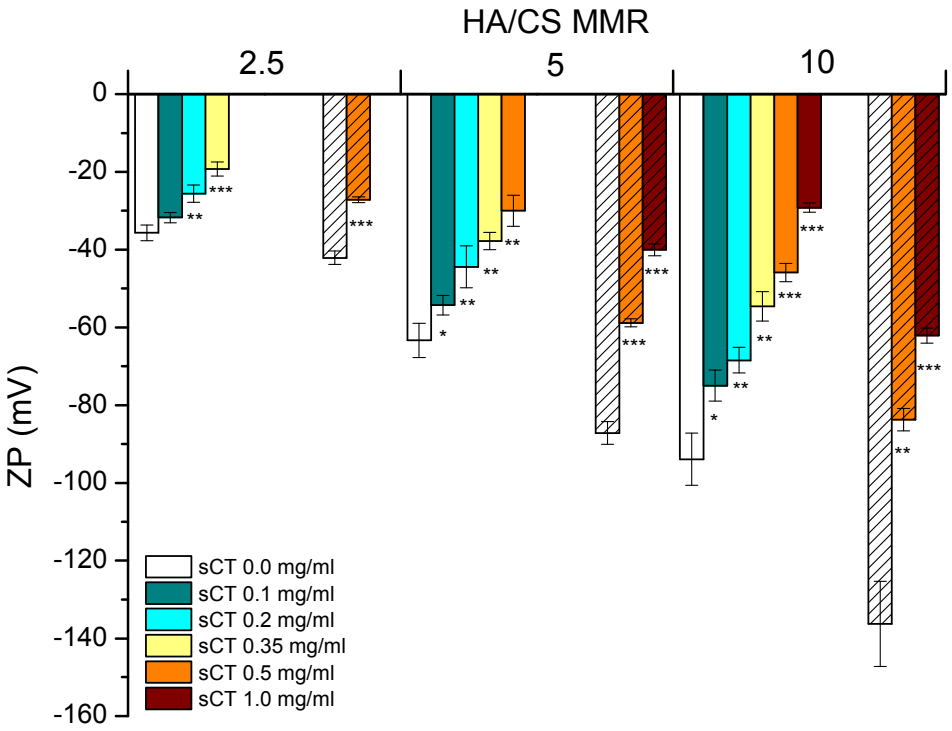
HA/CS MMR
2.5
5
10
ZP (mV)
0
-20
-40
-60
-80
-100
-120
-140
-160
sCT 0.0 mg/ml
sCT 0.1 mg/ml
sCT 0.2 mg/ml
sCT 0.35 mg/ml
sCT 0.5 mg/ml
sCT 1.0 mg/ml

Figure 7.

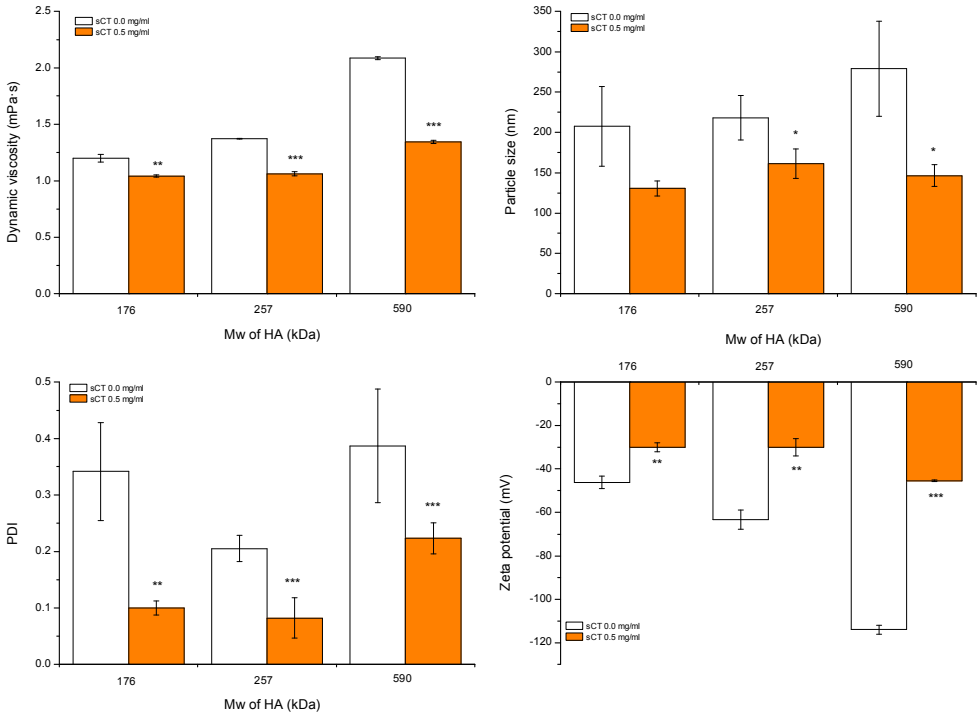
sCT 0.0 mg/ml
sCT 0.5 mg/ml
Dynamic viscosity (mPa·s)
Particle size (nm)
PDI
Zeta potential (mV)
Mw of HA (kDa)
176
257
590
**
***
*

Figure 8.

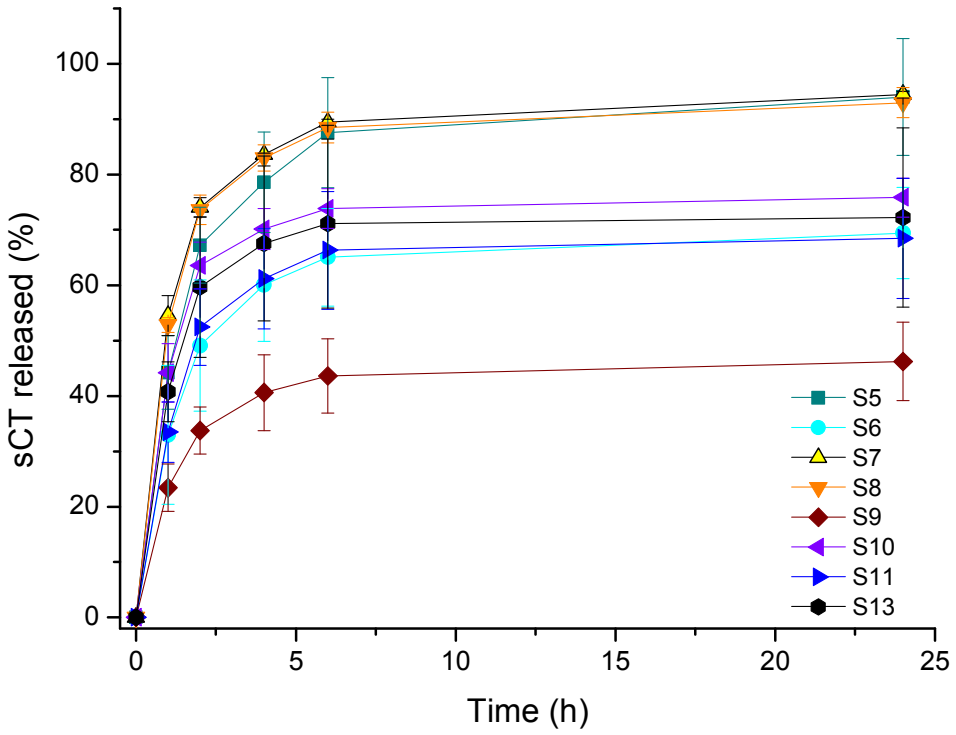
sCT released (%)
Time (h)
0
20
40
60
80
100
0
5
10
15
20
25
S5
S6
S7
S8
S9
S10
S11
S13

Figure 9.